

Shell model studies of the proton drip line nucleus ^{106}Sb

T. Engeland, M. Hjorth-Jensen and E. Osnes

Department of Physics, University of Oslo, N-0316 Oslo, Norway

We present results of shell model calculations for the proton drip line nucleus ^{106}Sb . The shell model calculations were performed based on an effective interaction for the $2s1d0g_{7/2}0h11_{11/2}$ shells employing modern models for the nucleon-nucleon interaction. The results are compared with the recently proposed experimental yrast states. A good agreement with experiment is found lending support to the experimental spin assignments.

PACS number(s): 21.60.-n, 21.60.Cs, 27.60.+j

Considerable attention is at present being devoted to the experimental and theoretical study of nuclei close to the limits of stability. Recently, heavy neutron deficient nuclei in the mass regions of $A = 100$ have been studied, and nuclei like ^{100}Sn and neighboring isotopes have been identified [1–3]. Moreover, the proton drip line has been established in the $A = 100$ and $A = 150$ regions [4] and nuclei like ^{105}Sb and ^{109}I have recently been established as ground-state proton emitters [5,6]. The next to drip line nucleus for the antimony isotopes, ^{106}Sb with a proton separation energy of ~ 400 keV, was studied recently in two experiments and a level scheme for the yrast states was proposed in Ref. [7].

The aim of this work is thus to see whether shell-model calculations, which employ realistic effective interactions based on state of the art models for the nucleon-nucleon interaction, are capable of reproducing the experimental results for systems close to the stability line. Before we present our results, we will briefly review our theoretical framework. In addition, we present results for effective proton and neutron charges based on perturbative many-body methods. These effective charges will in turn be used in a shell-model analysis of $E2$ transitions.

The aim of microscopic nuclear structure calculations is to derive various properties of finite nuclei from the underlying hamiltonian describing the interaction between nucleons. We derive an appropriate effective two-body interaction for valence neutrons and protons in the single-particle orbits $2s_{1/2}$, $1d_{5/2}$, $1d_{3/2}$, $0g_{7/2}$ and $0h_{11/2}$. As closed shell core we use ^{100}Sn . This effective two-particle interaction is in turn used in the shell model model study of ^{106}Sb . The shell model problem requires the solution of a real symmetric $n \times n$ matrix eigenvalue equation

$$\tilde{H} |\Psi_k\rangle = E_k |\Psi_k\rangle, \quad (1)$$

with $k = 1, \dots, K$. At present our basic approach to finding solutions to Eq. (1) is the Lanczos algorithm, an iterative method which gives the solution of the lowest eigenstates. The technique is described in detail in Ref. [8], see also Ref. [9].

To derive the effective interaction, we employ a perturbative many-body scheme starting with the free nucleon-nucleon interaction. This interaction is in turn renormalized taking into account the specific nuclear medium.

The medium renormalized potential, the so-called G -matrix, is then employed in a perturbative many-body scheme, as detailed in Ref. [10] and reviewed briefly below. The bare nucleon-nucleon interaction we use is the charge-dependent meson-exchange model of Machleidt and co-workers [11], the so-called CD-Bonn model. The potential model of Ref. [11] is an extension of the one-boson-exchange models of the Bonn group [12], where mesons like π , ρ , η , δ , ω and the fictitious σ meson are included. In the charge-dependent version of Ref. [11], the first five mesons have the same set of parameters for all partial waves, whereas the parameters of the σ meson are allowed to vary.

The first step in our perturbative many-body scheme is to handle the fact that the repulsive core of the nucleon-nucleon potential V is unsuitable for perturbative approaches. This problem is overcome by introducing the reaction matrix G given by the solution of the Bethe-Goldstone equation

$$G = V + V \frac{Q}{\omega - QTQ} G, \quad (2)$$

where ω is the unperturbed energy of the interacting nucleons, and H_0 is the unperturbed hamiltonian. The operator Q , commonly referred to as the Pauli operator, is a projection operator which prevents the interacting nucleons from scattering into states occupied by other nucleons. In this work we solve the Bethe-Goldstone equation for five starting energies ω , by way of the so-called double-partitioning scheme discussed in e.g., Ref. [10]. A harmonic-oscillator basis was chosen for the single-particle wave functions, with an oscillator energy $\hbar\Omega$ given by $\hbar\Omega = 45A^{-1/3} - 25A^{-2/3} = 8.5$ MeV, $A = 100$ being the mass number.

Finally, we briefly sketch how to calculate an effective two-body interaction for the chosen model space in terms of the G -matrix. Since the G -matrix represents just the summation to all orders of ladder diagrams with particle-particle intermediate states, there are obviously other terms which need to be included in an effective interaction. Long-range effects represented by core-polarization terms are also needed. The first step then is to define the so-called \hat{Q} -box given by

$$P\hat{Q}P = PGP + P\left(G\frac{Q}{\omega-H_0}G + G\frac{Q}{\omega-H_0}G\frac{Q}{\omega-H_0}G + \dots\right)P. \quad (3)$$

The \hat{Q} -box is made up of non-folded diagrams which are irreducible and valence linked. The projection operators P and Q define the model space and the excluded space, respectively, with $P + Q = I$. All non-folded diagrams through third order in the interaction G are included in the definition of the \hat{Q} -box while so-called folded diagrams are included to infinite order through the summation scheme discussed in Refs. [10,13].

Effective interactions based on the CD-Bonn nucleon-nucleon interaction have been used by us for several mass regions, and give in general a very good agreement with the data, see Refs. [14–17].

In addition to deriving an effective interaction for the shell model, we present also effective proton and neutron charges based on our perturbative many-body methods. These charges are used in our studies of available $E2$ data below. In this way, degrees of freedom not accounted for by the shell-model space are partly included through the introduction of an effective charge. The effective single-particle operators for the effective charge are calculated along the same lines as the effective interaction. In nuclear transitions, the quantity of interest is the transition matrix element between an initial state $|\Psi_i\rangle$ and a final state $|\Psi_f\rangle$ of an operator \mathcal{O} (here it is the $E2$ operator) defined as

$$\mathcal{O}_{fi} = \frac{\langle\Psi_f|\mathcal{O}|\Psi_i\rangle}{\sqrt{\langle\Psi_f|\Psi_f\rangle\langle\Psi_i|\Psi_i\rangle}}. \quad (4)$$

Since we perform our calculation in a reduced space, the exact wave functions $\Psi_{f,i}$ are not known, only their projections $\Phi_{f,i}$ onto the model space. We are then confronted with the problem of evaluating \mathcal{O}_{fi} when only the model space wave functions are known. In treating this problem, it is usual to introduce an effective operator \mathcal{O}_{eff} different from the original operator \mathcal{O} defined by requiring

$$\mathcal{O}_{fi} = \langle\Phi_f|\mathcal{O}_{\text{eff}}|\Phi_i\rangle. \quad (5)$$

The standard scheme is then to employ a perturbative expansion for the effective operator, see e.g. Refs. [18–20].

To obtain effective charges, we evaluate all effective operator diagrams through second-order, excluding Hartree-Fock insertions, in the G -matrix obtained with the CD-Bonn interaction. Such diagrams are discussed in the reviews by Towner [18] and Ellis and Osnes [19]. The state dependent effective charges are listed in Table I for the diagonal contributions only. In order to reproduce the experimental $B(E2; 4_1^+ \rightarrow 2_1^+)$ transition of Ref. [7], the authors introduced effective charges $e_p = 1.72e$ and $e_n = 1.44e$ for protons and neutrons, respectively. We see from Table I that the microscopically calculated values differ significantly from the above values from Ref. [7]. This could however very well be an artefact of the

chosen model space and effective interaction employed in the shell model analysis of Ref. [7]. The reader should also keep in mind that our model for the single-particle wave functions, namely the harmonic oscillator, may not be the most appropriate for the proton single-particle states, since the proton separation energy is of the order of some few keV. When compared with the theoretical calculation of Sagawa *et al.* [21], our neutron effective charges agree well with theirs, whereas the proton effective charge deduced in Ref. [21] is slightly larger, $e_p \sim 1.4e$. We note also that in the Hartree-Fock calculation with a Skyrme interaction and accounting for effects from the continuum, Hamamoto and Sagawa [22] obtained effective charges of $e_n = 1.35e$ and $e_p = 1.0e$ for ^{100}Sn . Below we will allow the effective charges to vary in order to reproduce as far as possible the experimental value of $2.8(3)$ W.u. for the transition $B(E2; 4_1^+ \rightarrow 2_1^+)$. There we will also relate the theoretical values for the effective charges to those extracted from data around $A = 100$, see e.g., Ref. [23].

The calculations were performed with two possible model spaces, one which comprises all single-particle orbitals of the $1d_{5/2}0g_{7/2}1d_{3/2}2s_{1/2}0h_{11/2}$ shell and one which excludes the $0h_{11/2}$ orbit. The latter model space was employed by the authors of Ref. [7] in their shell model studies. Since the single-neutron and single-proton energies with respect to ^{100}Sn are not well-established, we have adopted for neutrons the same single-particle energies as used in large-scale shell-model calculations of the Sn isotopes, see Refs. [15]. The neutron single-particle energies are $\varepsilon_{0g_{7/2}} - \varepsilon_{1d_{5/2}} = 0.2$ MeV, $\varepsilon_{1d_{3/2}} - \varepsilon_{1d_{5/2}} = 2.55$ MeV, $\varepsilon_{2s_{1/2}} - \varepsilon_{1d_{5/2}} = 2.45$ MeV and $\varepsilon_{0h_{11/2}} - \varepsilon_{1d_{5/2}} = 3.2$ MeV. These energies, when employed with our effective interaction described above, gave excellent results for both even and odd tin isotopes from ^{102}Sn to ^{116}Sn . The proton single-particle energies are less established and we simply adopt those for the neutrons. Since the proton separation energy is of the order of ~ 400 keV, it should suffice to carry out a shell-model calculation with just the $1d_{5/2}0g_{7/2}$ orbits for protons. The total wave function, see the discussion below, is however to a large extent dominated by the $1d_{5/2}$ orbital for protons, with small admixtures from the $0g_{7/2}$ proton orbital. The influence from the other proton orbits is thus minimal.

The resulting eigenvalues are displayed in Fig. 1 for the two choices of model space together with the experimental levels reported in Ref. [7]. Not all experimental levels have been given a spin assignment and all experimental spin values are tentative. The label FULL stands for the model space which includes all orbits from the $1d_{5/2}0g_{7/2}1d_{3/2}2s_{1/2}0h_{11/2}$ shell while REDUCED stands for the model space where the $0h_{11/2}$ orbit has been omitted. As can be seen from Fig. 1, the agreement with experiment is also rather good, with the model space which includes all orbitals of the $1d_{5/2}0g_{7/2}1d_{3/2}2s_{1/2}0h_{11/2}$ shells being closest to the experimental level assignments. The reader should how-

ever note that in Ref. [7] it is not excluded that the ground state could have spin 1^+ , which means that the experimental spin values in Fig. 1 should be reduced by 1. In our theoretical calculations we obtain in addition to a state with spin 1^+ , also a state with 3^+ not seen in the experiment of Ref. [7]. In case the ground state turns out to have spin 1^+ , the reduced model space in our calculations would yield a better agreement with the data.

The wave functions for the various states are to a large extent dominated by the $0g_{7/2}$ and $1d_{5/2}$ single-particle orbits for neutrons (ν) and the $1d_{5/2}$ single-particle orbit for protons (π). The $\nu 0g_{7/2}$ and $\nu 1d_{5/2}$ single-particle orbits represent in general more than $\sim 90\%$ of the total neutron single-particle occupancy, while the $\pi 1d_{5/2}$ single-particle orbits stands for $\sim 80 - 90\%$ of the proton single-particle occupancy. The other single-particle orbits play an almost negligible role in the structure of the wave functions. The only notable exception is the 7_1^+ state where $\pi 0g_{7/2}$ stands for the 84% of the proton single-particle occupancy. This has also important repercussions on the contributions to the measured $E2$ transition $B(E2; 4_1^+ \rightarrow 2_1^+)$, where the structure of the wave functions of the 4_1^+ and 2_1^+ states are to a large extent dominated by the $\nu 1d_{5/2}$ and $\pi 1d_{5/2}$ single-particle orbits. The $0g_{7/2}$ orbits play a less significant role in the structure of the wave functions, and since the $0g_{7/2} \leftrightarrow 1d_{5/2}$ transition matrix element tends to be weaker than the one between $1d_{5/2} \leftrightarrow 1d_{5/2}$, the $E2$ transition will be dominated by the latter contributions. As also noted by Sohler *et al.* [7], the $E2$ transition is dominated by neutron contributions. This can also be seen from Fig. 2 where we show the result for the above $E2$ transition as function of different choices for the effective charges. We see that the largest change in the value of the $E2$ transition takes place when we vary the effective charge of the neutron, whereas when the proton charge is changed, the percentual change is smaller. Furthermore, if we use the largest values for effective charges of Table I, namely $e_n = 0.72e$ and $e_p = 1.16e$, we obtain 1.84 W.u. for the $E2$ transition. Compared with the experimental value of 2.8(3) W.u. this may indicate that both the proton and the neutron effective charges should be slightly increased. From Fig. 2 we see that effective charges of $e_n = 0.9e$ and $e_p = 1.4e \pm 0.2e$ seem to yield the best agreement with experiment, although neutron charges of $e_n = 0.8e$ and $e_n = 1.0e$ yield results within the experimental window of Fig. 2. The neutron effective charges would agree partly with those extracted from the data in the Sn isotopes [21] and from theoretical calculations of $E2$ transitions in heavy Sn isotopes [15], where a value $e_n \sim 1$ is adopted in order to reproduce the data. The calculated effective charges of Table I are however on the lower side. However, the deduced effective charges from the $B(E2; 6_1^+ \rightarrow 4_1^+)$ transitions in ^{102}Sn [23] and ^{104}Sn [24] indicate that $e_n \sim 1.6 - 2.3e$, depending on the effective interaction employed in the shell-model analyses. Clearly, the effective interaction

which is used, and its pertinent model space, approximations made in the many-body formalism etc., will influence the extraction of effective charges. This notable difference in the effective charges could be due to the fact that the $B(E2; 6_1^+ \rightarrow 4_1^+)$ transitions in ^{102}Sn and ^{104}Sn involve configurations not accounted for by the $1d_{5/2}0g_{7/2}1d_{3/2}2s_{1/2}0h_{11/2}$ model space. A proton effective charge of $e_p \sim 1.4e$ is close to values inferred from experiment for the $N = 50$ isotones, see Ref. [1,2], shell-model calculations of $E2$ transitions for the $N = 82$ isotones [25] and the theoretical estimates of Ref. [21].

In summary, a shell-model calculation with realistic effective interactions of the newly reported low-lying yrast states of the proton drip line nucleus ^{106}Sb , reproduces well the experimental data. Since the wave functions of the various states are to a large extent dominated by neutronic degrees of freedom and neutrons are well bound with a separation energy of ~ 8 MeV, this may explain why a shell-model calculation, within a restricted model space for a system close to the proton drip line, gives a satisfactory agreement with the data. In order to reproduce the experimental $B(E2; 4_1^+ \rightarrow 2_1^+)$ transition, we obtained effective charges from our shell-model wave functions of $e_n = 0.8 - 1.0e$ and $e_p = 1.4e \pm 0.2e$. Our microscopically calculated effective charges are however slightly smaller, $e_n = 0.5 - 0.7e$ and $e_p = 1.1 - 1.2e$.

-
- [1] M. Lipoglavsek *et al.*, Phys. Rev. Lett. **76**, 888 (1996).
 - [2] M. Gorska *et al.*, Phys. Rev. Lett. **79**, 2415 (1997).
 - [3] H. Grawe *et al.*, Z. Phys. **A358**, 185 (1997).
 - [4] P. J. Woods and C. N. Davids, Annu. Rev. Nucl. Sci. **47**, 541 (1997).
 - [5] R. J. Tighe, D. M. Moltz, J. C. Batchelder, T. J. Ognibene, M. W. Rowe, and J. Cerny, Phys. Rev. C **49**, R2871 (1994).
 - [6] C. -H. Yu *et al.*, Phys. Rev. C **59**, R1834 (1999).
 - [7] D. Sohler *et al.*, Phys. Rev. C **59**, 1324 (1999).
 - [8] R. R. Whitehead, A. Watt, B. J. Cole, and I. Morrison, Adv. Nucl. Phys. **9**, 123 (1977).
 - [9] T. Engeland, M. Hjorth-Jensen, A. Holt, and E. Osnes, Phys. Scripta **T56**, 58 (1995).
 - [10] M. Hjorth-Jensen, T. T. S. Kuo, and E. Osnes, Phys. Rep. **261**, 125 (1995).
 - [11] R. Machleidt, F. Sammarruca, and Y. Song, Phys. Rev. C **53**, 1483 (1996).
 - [12] R. Machleidt, Adv. Nucl. Phys. **19**, 189 (1989).
 - [13] T. T. S. Kuo and E. Osnes, Folded-Diagram Theory of the Effective Interaction in Atomic Nuclei, Springer Lecture Notes in Physics, (Springer, Berlin, 1990) Vol. 364.
 - [14] G. N. White *et al.*, Nucl. Phys. **A644**, 277 (1998).
 - [15] A. Holt, T. Engeland, M. Hjorth-Jensen, and E. Osnes, Nucl. Phys. **A634**, 41 (1998).
 - [16] T. Siiskonen, J. Suhonen, and M. Hjorth-Jensen, Phys. Rev. C **59**, R1839 (1999).

- [17] D. J. Dean, M. T. Ressel, M. Hjorth-Jensen, S. E. Koonin, K. Langanke, and A. Zuker, Phys. Rev. C **59**, (1999), in press.
- [18] I. S. Towner, Phys. Rep. **155**, 263 (1987).
- [19] P.J. Ellis and E. Osnes, Rev. Mod. Phys. **49**, 777 (1977).
- [20] E. M. Krenciglowa, T. T. S. Kuo, E. Osnes, and P. J. Ellis, Nucl. Phys. **A289**, 381 (1977).
- [21] H. Sagawa, O. Scholten, B. A. Brown, and B. H. Wildenthal, Nucl. Phys. **A462**, 1 (1987).
- [22] I. Hamamoto and H. Sagawa, Phys. Lett. **B394**, 1 (1997).
- [23] M. Lipoglavsek, PhD. Thesis, University of Lund (1998), unpublished; M. Lipoglavsek *et al.*, Phys. Lett. **B440**, 246 (1998).
- [24] R. Schubart *et al.*, Z. Phys. **A352**, 373 (1995).
- [25] A. Holt, T. Engeland, M. Hjorth-Jensen, E. Osnes, and

J. Suhonen, Nucl. Phys. **A618**, 107 (1997).

TABLE I. Proton and neutron effective charges relative to ^{100}Sn for the $1d_{5/2}$, $0g_{7/2}$, $1d_{3/2}$, $2s_{1/2}$ and $0h_{11/2}$ single particle orbitals.

	Proton	Neutron
$1d_{5/2}$	1.06e	0.53e
$0g_{7/2}$	1.15e	0.72e
$1d_{3/2}$	1.04e	0.52e
$0h_{11/2}$	1.16e	0.51e

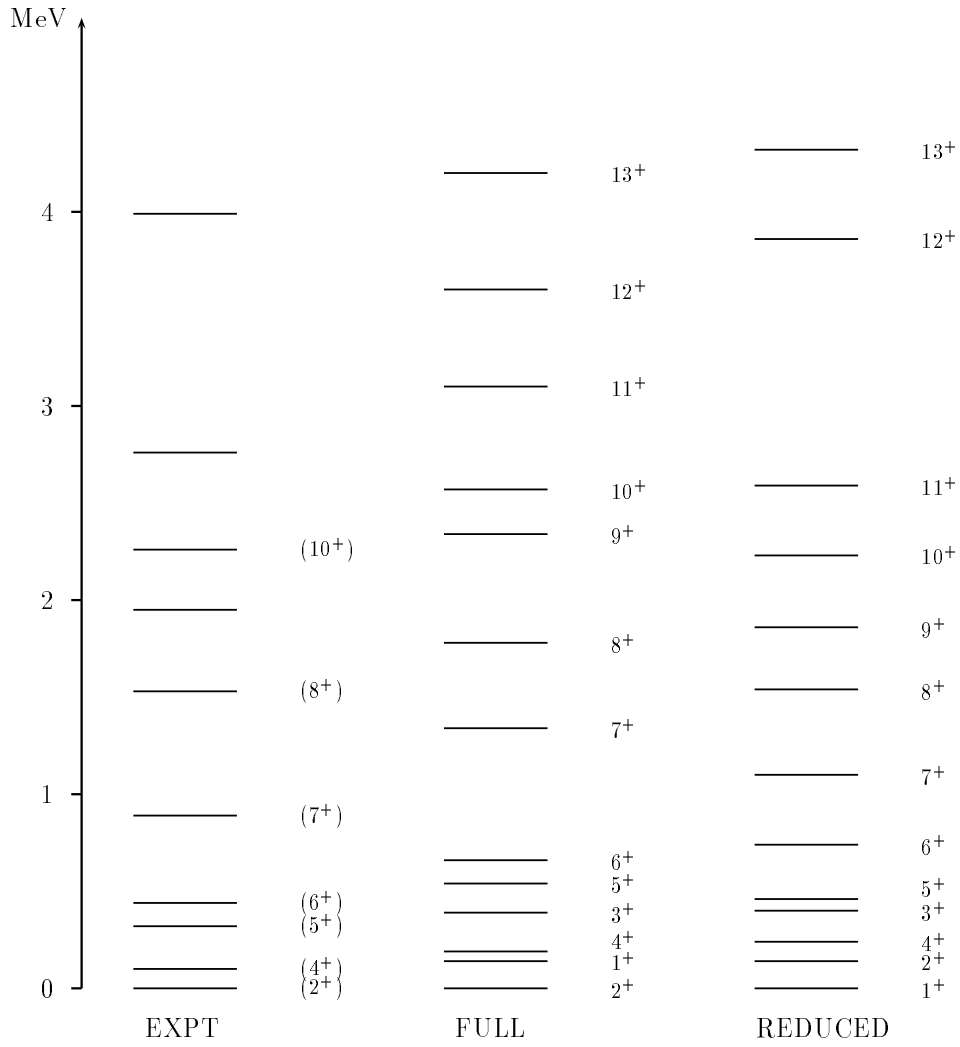


FIG. 1. Low-lying states for ^{106}Sb , theory and experiment. Energies in MeV. FULL means the model space which comprises all single-particle orbits, $2s1d0g_{7/2}0h11_{11/2}$. REDUCED means that the $0h11_{11/2}$ single-particle orbit is not included.

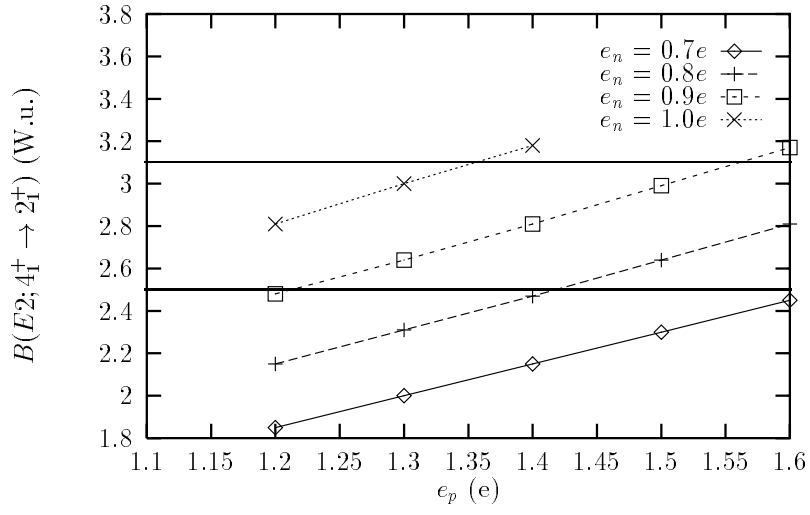


FIG. 2. Value for the $B(E2; 4_1^+ \rightarrow 2_1^+)$ transition as function of different effective charges in units of W.u. The horizontal lines represent the experimental window, with a value of 2.8 ± 0.3 W.u.